

Electronic Supplementary Information

Ultrathin tungsten-doped hydrogenated titanium dioxide nanosheets for solar-driven hydrogen evolution

Xiaoyu Chen, Zhi Han, Bojing Sun, Yu Wang, Xijiang Han*, and Ping Xu*

MIIT Key Laboratory of Critical Materials Technology for New Energy Conversion and Storage, School of Chemistry and Chemical Engineering, Harbin Institute of Technology, Harbin 150001, China

Email: pxu@hit.edu.cn (P.X.); hanxijiang@hit.edu.cn (X.H.)

Contents

Fig. S1	Optical photos of W-h-TiO ₂ and h-TiO ₂ nanosheets.	3
Fig. S2	XRD pattern and TEM image of W ₂ C nanoparticles.	3
Fig. S3	AFM images and corresponding height profiles of W-h-TiO ₂ nanosheets and h-TiO ₂ nanosheets.	4
Fig. S4	Full XPS scan spectra of W-h-TiO ₂ nanosheets.	4
Fig. S5	W 4d XPS spectra of W-h-TiO ₂ nanosheets.	5
Fig. S6	C 1s XPS spectra of W-h-TiO ₂ nanosheets.	5
Fig. S7	Optical bandgap of pure h-TiO ₂ and W-h-TiO ₂ nanosheets.	5
Fig. S8	Mott-Schottky plots under different frequency of W-h-TiO ₂ nanosheets and pure h-TiO ₂ nanosheets.	6
Fig. S9	UPS spectra of h-TiO ₂ and W-h-TiO ₂ nanosheets.	6
Fig. S10	H ₂ evolution rates of W-h-TiO ₂ nanosheets under constant temperature of 25 °C.	7
Fig. S11.	H ₂ evolution rates of W-h-TiO ₂ nanosheets with 0.5wt% H ₂ PtCl ₆ as cocatalyst.	7
Table. S1	Actual molar ratio of W to Ti in W-h-TiO ₂ nanosheets measured by ICP-OES.	8
Table. S2	Time-resolved PL decay curve parameters obtained by double-exponential function simulation.	8
Table. S3	Photocatalytic hydrogen production performance of photocatalysts reported in literatures.	8

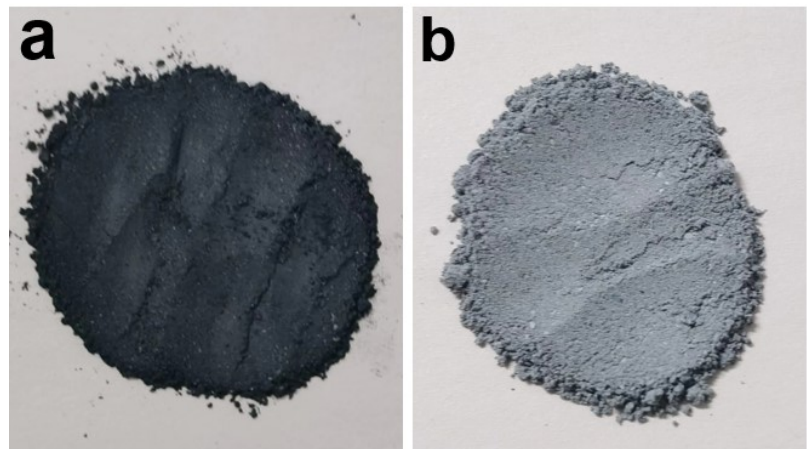


Fig. S1. Optical photos of (a) W-h-TiO₂ nanosheets and (b) h-TiO₂ nanosheets.

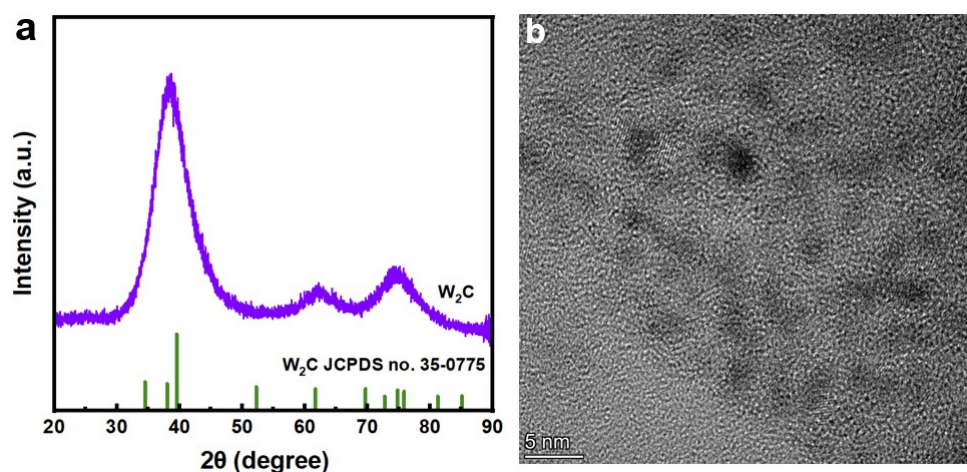


Fig. S2. (a) XRD pattern and (b) TEM image of W₂C nanoparticles.

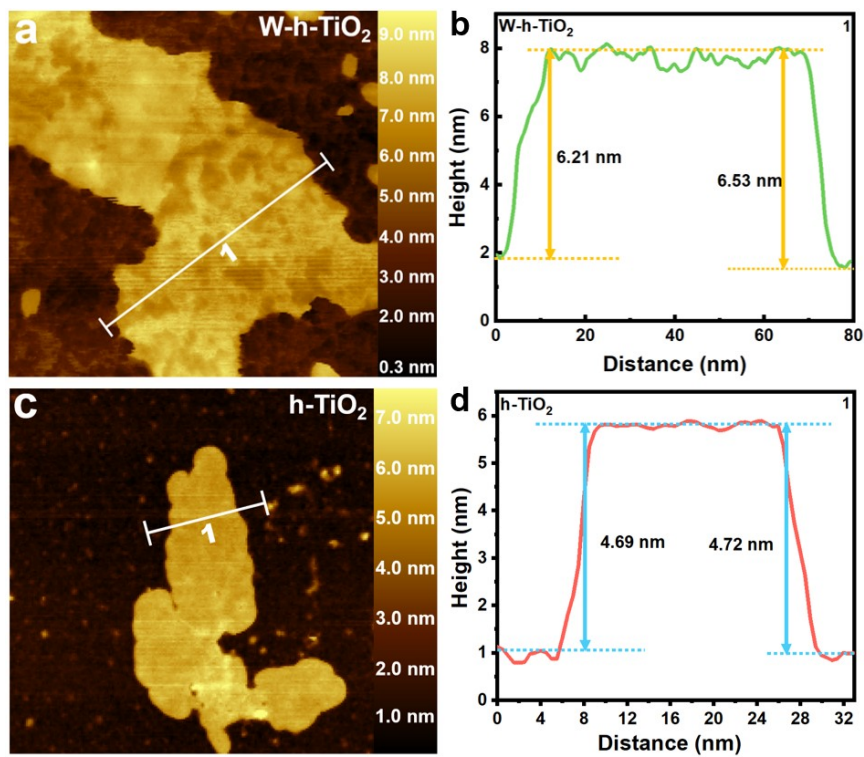


Fig. S3. (a, c) AFM images and (b, d) corresponding height profiles of W-h-TiO₂ nanosheets and h-TiO₂ nanosheets.

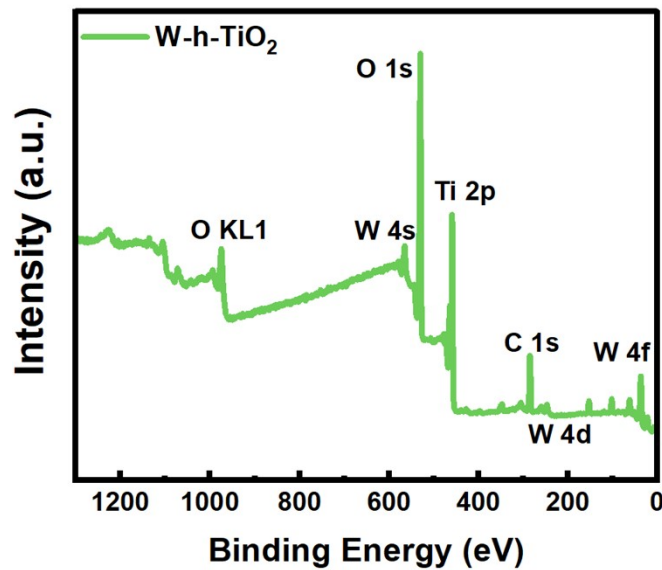


Fig. S4. Full XPS scan spectrum of W-h-TiO₂ nanosheets.

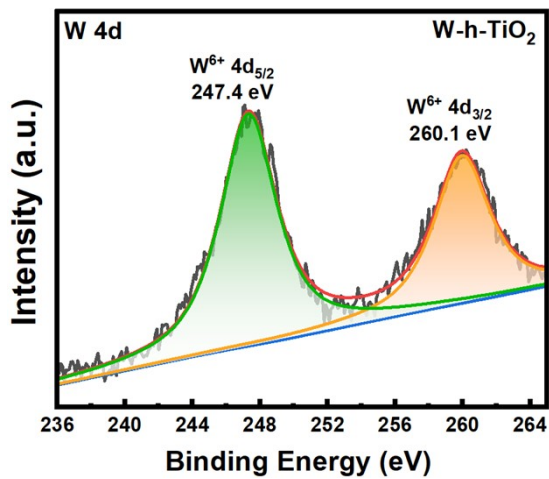


Fig. S5. W 4d XPS spectrum of W-h-TiO₂ nanosheets.

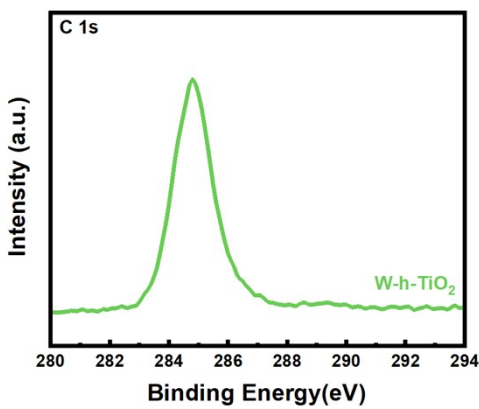


Fig. S6. C 1s XPS spectrum of W-h-TiO₂ nanosheets.

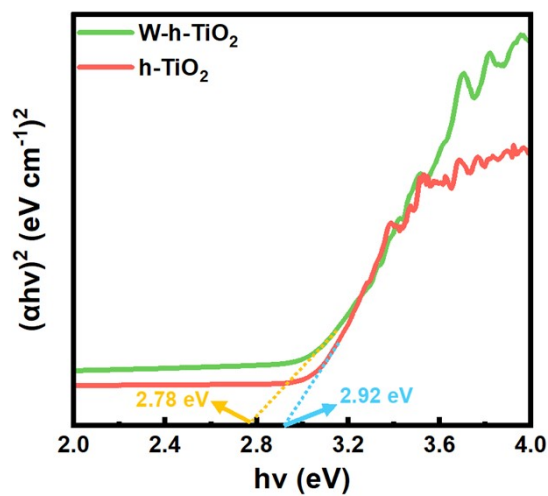


Fig. S7. Optical bandgap of pure h-TiO₂ and W-h-TiO₂ nanosheets.

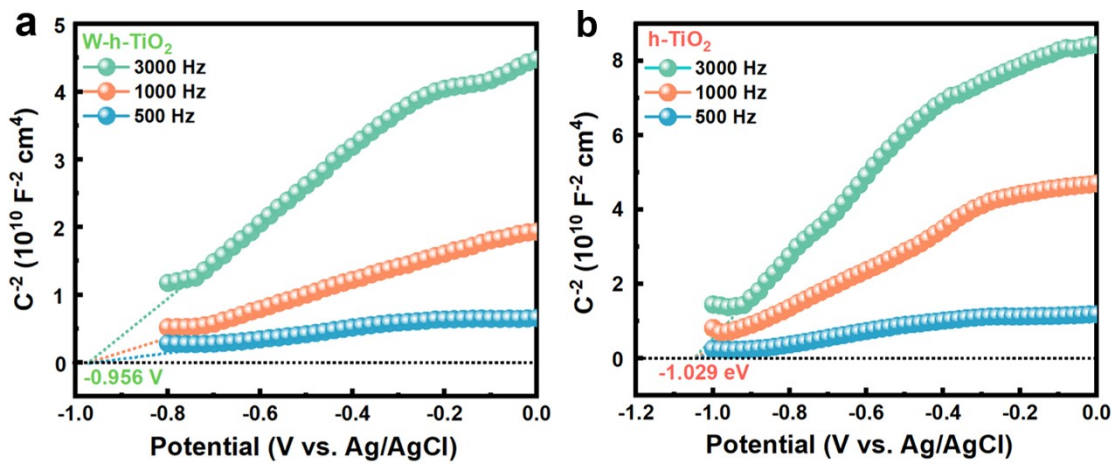


Fig. S8. Mott-Schottky plots under different frequency of (a) W-h-TiO₂ nanosheets and (b) pure h-TiO₂ nanosheets.

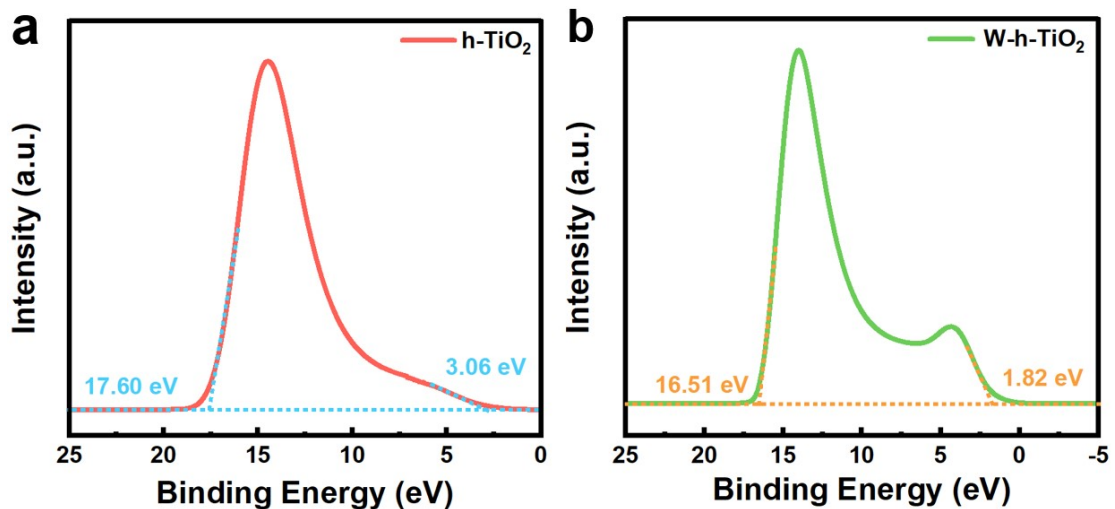


Fig. S9. UPS spectra of (a) h-TiO₂ nanosheets and (b) W-h-TiO₂ nanosheets.

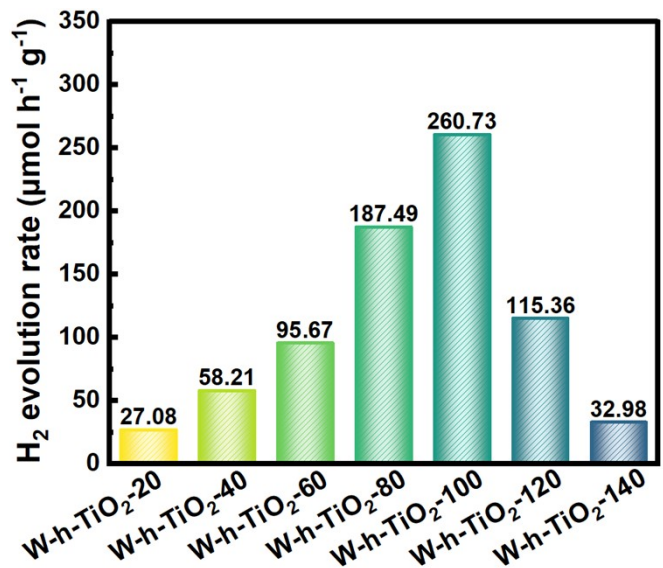


Fig. S10. H_2 evolution rates of W-h-TiO₂ nanosheets under a constant temperature of 25 °C.

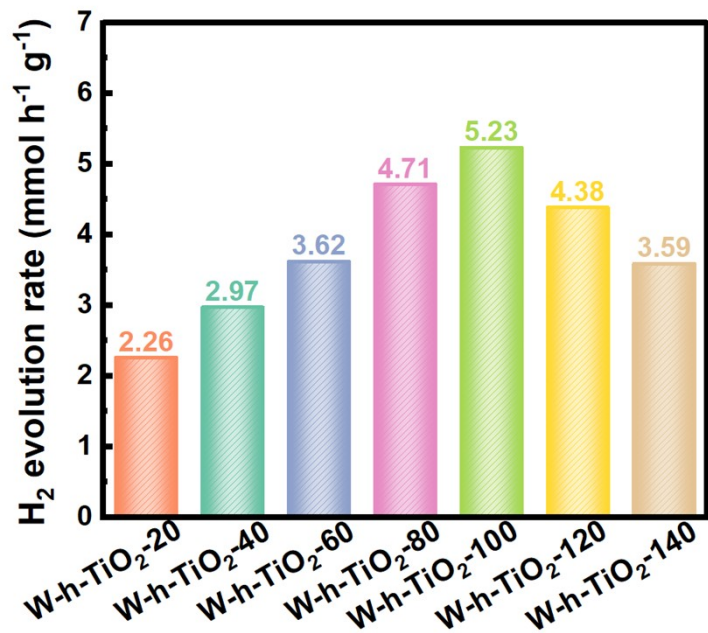


Fig. S11. H_2 evolution rates of W-h-TiO₂ nanosheets with 0.5wt% H₂PtCl₆ as cocatalyst.

Table S1. Actual molar ratio of W to Ti in W-h-TiO₂ nanosheets measured by ICP-OES.

Samples	molar ratio of W to Ti
W-h-TiO ₂ -20	0.27%
W-h-TiO ₂ -40	0.58%
W-h-TiO ₂ -60	0.93%
W-h-TiO ₂ -80	1.35%
W-h-TiO ₂ -100	1.77%
W-h-TiO ₂ -120	2.18%
W-h-TiO ₂ -140	2.69%

Table S2. Time-resolved PL decay curve parameters obtained by double-exponential function simulation.

samples	τ_1 (ns)	τ_2 (ns)	A ₁ (%)	A ₂ (%)	τ_{ave} (ns)
h-TiO ₂	2.71	22.61	85.92	14.08	5.52
W-h-TiO ₂	3.97	58.36	67.62	32.38	21.58

Table S3. Photocatalytic hydrogen production performance of photocatalysts reported in literatures.

Photocatalysts	H ₂ (mmol/g/h)	Illumination	Sacrificial agent	Ref.
Ru-TiO ₂	0.85	300 W Xe lamp (AM 1.5G)	3wt% Ru and 20 mL CH ₃ OH	1
Pt/Ga-TiO ₂	5.122	300 W Xe lamp (AM 1.5G)	0.5wt% H ₂ PtCl ₆ and 20 mL CH ₃ OH	2
Fe-Ni/Ag/TiO ₂	0.793	300 W Xe lamp (AM 1.5G)	20 mL CH ₃ OH	3
S-TiO ₂	163.9	300 W Xe lamp (AM 1.5G)	20 mL CH ₃ OH	4
N-TiO ₂ /Pt	0.57	300 W Xe lamp (AM 1.5G)	20 mL CH ₃ OH	5
Ni/TiO ₂	3.39	300 W Xe lamp (AM 1.5G)	1wt% H ₂ PtCl ₆ and 20 mL CH ₃ OH	6
Cu-mpTiO ₂	1.00	300 W Xe lamp (AM 1.5G)	1wt% H ₂ PtCl ₆ and 20 mL CH ₃ OH	7
1T-WS₂/2H-WS₂/CdS	5.23	300 W Xe lamp (AM 1.5G)	0.5wt% H₂PtCl₆ and 20 mL CH₃OH	This work

References

1. W. Ouyang, M. J. Munoz-Batista, A. Kubacka, R. Luque, M. Fernández-García, Enhancing photocatalytic performance of TiO₂ in H₂ evolution via Ru co-catalyst deposition, *Appl. Catal. B*, 2018, **238**, 434-443.
2. S. Luo, T. D. Nguyen-Phan, D. Vovchok, I. Waluyo, R. M. Palomino, A. D. Gamlski, L. Barrio, W. Xu, D.E. Polyansky, J.A. Rodriguez, Enhanced, robust light-driven H₂ generation by gallium-doped titania nanoparticles, *Phys. Chem. Chem. Phys.*, 2018, **20**, 2104-2112.
3. T. Sun, E. Z. Liu, X. H. Liang, X. Y. Hu, J. Fan, Enhanced hydrogen evolution from water splitting using Fe-Ni codoped and Ag deposited anatase TiO₂ synthesized by solvothermal method, *Appl. Surf. Sci.*, 2015, **347**, 696-705.
4. Z. P. Xing, Z. Z. Li, X. Y. Wu, G. F. Wang, W. Zhou, In-situ S-doped porous anatase TiO₂ nanopillars for high-efficient visible-light photocatalytic hydrogen evolution, *Int. J. Hydrogen Energy*, 2016, **41**, 1535-1541.
5. B. S. Huang, M. Y. Wey, Properties and H₂ production ability of Pt photodeposited on the anatase phase transition of nitrogen-doped titanium dioxide, *Int. J. Hydrogen Energy*, 2011, **36**, 9479-9486.
6. F. Wu, X. Y. Hu, J. Fan, E. Z. Liu, T. Sun, L. M. Kang, W. Q. Hou, C. J. Zhu, H. C. Liu, Photocatalytic activity of Ag/TiO₂ nanotube arrays enhanced by surface plasmon resonance and application in hydrogen evolution by water splitting, *Plasmonics*, 2013, **8**, 501-508.
7. R. A. Rather, S. Singh, B. Pal, A Cu⁺¹/Cu⁰-TiO₂ mesoporous nanocomposite exhibits improved H₂ production from H₂O under direct solar irradiation, *J. Catal.*, 2017, **346**, 1-9.